Vol. 7 | 20 | International Journal of
Nº 1 | 20 | Medical and Surgical Sciences

UNIVERSIDAD AUTONOMA DE CHILE

Article

A NOVEL APPROACH FOR PRE-SURGICAL EVALUATION OF FACIAL MORPHOMETRY IN CHILDREN USING MAGNETIC RESONANCE IMAGING SCANS OF THE BRAIN: A FEASIBILITY ANALYSIS

Un enfoque novedoso para la evaluación prequirúrgica de la morfometría facial en niños mediante imágenes por resonancia magnética de cerebro: un análisis de viabilidad

Iroshani Kodikara
Department of Anatomy, Faculty of Medicine, University of Ruhuna, Sri Lanka.

Dhanusha Gamage
Provincial General Hospital, Rathnapura, Sri Lanka.

Gananda Nanayakkara
Department of Anatomy, Faculty of Medicine, University of Ruhuna, Sri Lanka.

Isurani Ilayperuma
Department of Anatomy, Faculty of Medicine, University of Ruhuna, Sri Lanka.

Corresponding author: *Iroshani Kodikara, Department of Anatomy, Faculty of Medicine, University of Ruhuna, Sri Lanka.*
E mail- iroshani.kodikara@gmail.com

Receipt: 29/06/2020
Acceptance: 02/09/2020

ABSTRACT

Pre-surgical evaluation of facial morphometry is frequently warranted for children with facial dysmorphism. Though many methods utilized previously for such purposes, data is scarce on using magnetic resonance (MRI) brain images for such purposes. The purpose of this study was to appraise the feasibility of utilizing MRI brain scans done in epilepsy imaging protocol to assess facial morphometry. Measurements of the face; orbit, mouth, and nose of children aged 1 to 7 years were obtained using T1 sagittal, T2 axial and three dimensional (3D) MRI images of the brain (n=20). Ability to obtain facial measurements, inter and intra-observer variability

calculated. The mean age of the studied children was 4±2 years, of which 40% (n=8) were boys, and 60% (n=12) were girls. Obtaining facial measurements were reliable with high intra-observer (α=0.757 to 0.999) and inter-observer agreements (α=0.823 to 0.997). The landmarks of the cranium, upper face, and upper nose could be identified (100%) in both two dimensional (2D) and 3D images when such landmarks were contained in the imaging field of view (FOV). Landmarks of lower nose, (subalar width = 0%) or mouth (0%) were not contained in the FOV of 2D images, but contained in 3D images (100%). Both 2D and 3D images did not allow assessment of lower face or the mandible as such landmarks were not contained in the FOV.

We conclude that Brain MRIs performed to evaluate cerebral pathology can be executed to assess facial measurements, provided the FOV of the scan is adjusted to include all significant landmarks.

Key words: Craniofacial malformations; children; facial measurements; feasibility; MRI brain.

1. Introduction

Facial appearance is a unique individual characteristic, hence is considered as the hallmark of personal identity (Johnston & Chazal, 2018). Among many facial features, features of the eyes, nose, and mouth bear the most distinctive personal characteristics (Johnston & Chazal, 2018). The graphs developed for electronic facial recognition systems evaluate the individual discriminative ability of the corners of the eyes and eyebrows; nasal tip, base of the nose, nasion; and the mouth (Çeliktutan, et al., 2013).

Facial reconstructive surgeries are warranted for both iatrogenic and congenital causes of facial disfiguration. The maximum cosmetic outcome of the surgeries is achieved through pre-surgical planning of the procedure that is usually done by examining unaffected facial landmarks and parameters. Often in gross facial dysmorphism, facial landmarks are profoundly distorted in both sides. Upon which, the facial reconstruction is aimed to maintain the facial symmetry (Chuang, et al., 2016).

Craniofacial abnormalities hallmark any congenital syndromes, such as craniofacial microsomia, Treacher Collins syndrome, Pierre Robin syndrome, and Nager syndrome (Paranaíba, et al., 2011). Among them, oro-facial cleft deformity is known to be the most prevalent. Oro-facial cleft encompasses a spectrum of malformations with many deformities such as combined cleft lip and palate; isolated cleft lip or palate; unilateral or bilateral involvement; incomplete or complete defects (Shkoukani, et al., 2013; Tettamanti & Avantaggiato, 2017). Depending on the severity of the malformation, the anatomy of various facial structures, such as perioral skin, orbicularis oris muscle, cupids bow and the philtrum of the upper lip, pre-maxillary bone and nasal structures are distorted to a varying degree. (Shkoukani, et al., 2013; Neiswanger, Weinberg, et al., 2007; Marazita, 2007). The surgical repair of oro-facial cleft deformity primarily aims to restore the normal anatomy and functional integrity (Shkoukani, et al., 2013; Campbell, et al., 2010; Ribeiro, et al., 2012).

Since the pre-surgical facial morphometric evaluation facilitates the outcome in facial reconstruction surgeries, several quantitative evaluation techniques have been used for many years. However, each of them was with advantages and disadvantages (Johnston & Chazal, 2018). The direct morphometric assessment that has been practiced over centuries is considered the gold standard. However, direct morphometry is time-consuming, and patient compliance is mandatory to obtain accurate results (Farkas,1994; Moss, et al.,1987). Facial morphometric evaluation using photographs has often resulted in measurement inaccuracies. Technique such as imprinting facial features in a mould is practically

inconvenient and traumatizing to the individual, therefore is not recommended for children (Othman, et al., 2016). Two-dimensional cephalometry has been used for years; however, exposure to ionizing radiation is hazardous, and image magnification leads to measurement inaccuracies (Farkas,1994; Moss, et al.,1987). Novel technologies, such as 3-dimensional methods and 3D printing of the face are rewarding; however, high cost and limited availability have made them less popular (de Menezes & Sforza, 2010). Three-dimensional image reconstruction using computed tomography exposes patients to ionizing radiation while providing poor resolution of surface landmarks (Farkas,1994).

Many syndromes with congenital facial dysmorphism are accompanied by intracranial abnormalities (Paranaíba, et al., 2011; Nopoulos, et al, 2007; Fakhim, et al., 2016). Therefore, intracranial imaging is often indicated to appraise the associated cerebral malformations. Out of many imaging modalities that offer reliable assessment of cerebral pathologies, the most suitable modality is selected by assessing the risks and benefits. Computed tomography (CT) offers satisfactory diagnostic yield in detecting brain abnormalities at the cost of exposure to ionizing radiation. The MRI is more sensitivity than CT in detecting structural brain abnormalities without exposing to ionizing radiation, hence, is considered as the gold standard imaging modality to investigate children with suspected brain abnormalities. Additionally, discrimination among soft tissue layers, such as skin, subcutaneous tissues, and muscles, is highest in MRI (David & Yousem, 2010; Reeth EV, et al., 2014). Further, MRI has been proven its validity in diagnosing a wide range of intracranial pathologies such as congenital cerebral anomalies, infarctions, and infections (David & Yousem, 2010; Reeth EV, et al., 2014).

Employing MRI for simultaneous assessment of cerebral and facial abnormalities would be safe, reliable and cost-effective. However, MRI brains that were performed to evaluate intra cerebral pathologies have not been evaluated previously for the feasibility of assessment of facial morphometry. Therefore, thinking along these lines, we hypothesized that the brain MRI studies performed to investigate suspected cerebral pathologies can successfully be used for pre-surgical definition of facial landmarks for facial reconstructions. Thus, the objectives of this study were to evaluate the feasibility and repeatability of using images of MRI brains performed in routine brain imaging protocol to assess the facial dimensions of children who require facial reconstruction surgeries and to propose the optimum MRI protocol that suits for such purposes.

2. Material and methods

This cross-sectional, observational, retrospective study has carried out beetween October 2019 to December 2019. The study has evaluated MRI brain images of twenty (n=20) children aged 1-7 years, of which 40% (n=8) were boys, and 60% (n=12) were girls. Measurements of orbit, mouth, and nose were obtained using magnetic resonance (MRI) scans of brain that were performed to investigate the etiology of epilepsy. As a pilot study, we evaluated a convenient number of samples to recommend a protocol for further evaluation. Past medical records were used to identify and exclude subjects with facial dysmorphism, microcephaly, growth abnormalities or craniofacial syndromes from the study. Age and gender of the subjects were recorded. Ethical approval for the study was obtained from the Ethical review committee (RP/2018/13).

MRI protocol

All the studied MRIs were done with Phillips Ingenia 3T Scanner released to the market in 2018. Out of all MRI brain sequences performed in routine epilepsy protocol, only following sequences were used to get the facial measurements: T1 weighted spin-echo (SE) sagittal sequence (TR- 420;

TE- 13); T2 weighted fast spin-echo (FSE) axial sequences (TR- 5680; TE-103); reconstructed three dimensional (3D) images from the above series. All brain scans were performed without injecting an intravenous contrast agent. In brain imaging protocol, the slice thickness was set at five millimeters (5 mm) and the field of views (FOV) of axial and sagittal scans were set as follows. The FOV of axial images extended from the vertex to base of the skull up to the line that joins the two mastoid processes; FOV of sagittal images extended from the anterior aspect of the face (including the tip of the nose in FOV) to the posterior aspect of the skull. The 3D image reconstruction was performed in sagittal images using electronic 3D reconstruction software of the scanner.

Obtaining facial measurements

The measurements required to assess facial morphometry were obtained from two dimensional (2D) sagittal and axial images and 3D MRI images. Phillips DICOM viewer image archiving software was used for image archiving. In the 2D MRI technique, measurements of the eyes, nose, and mouth were taken by a single experienced Radiologist, using the electronic measuring caliper of the image archiving software. The feasibility of obtaining measurements is defined as the ability to obtain measurements using defined landmarks. Each measurement was repeated thrice and the average considered for calculations. To evaluate the intra-observer variability measurements were repeated by the same investigator in a randomly selected sample (20% of the total study sample). Inter-observer variability was assessed by repeating the measurements (randomly selected -20%- sample from the entire study sample) by a second experienced Radiologist. The measurement bias has minimized as follows. The measurements were repeated under similar technical conditions; the same image-archiving software used for all measurements; both investigators were blind to previous measurements. To compare the accuracy of 2D and 3D methodologies, same measurements repeated in a randomly selected sample (20% of the total study sample) of 3D reconstructed images using 3D reconstruction software of the DICOM viewer.

Figure 1a defines the landmarks used to obtain the facial measurements. Bi-ocular width (BOW; 12 to 15), inter-ocular width (IOW; 13 to 14), right ocular width (ROW; 12 to 13), left ocular width (LOW; 14 to 15), right endo-cathion to nasion (REcN; 13 to 16), left endo-canthion to nasion (LEcN ; 14 to 16), alar base width (AlbW ; 9 to 10), pronasale to right alar base width (PronRlb; 9 to 11), pronasale to left alar base width (PronLlb ; 10 to 11), subalar width (6 to 8), mouth width (1 to 2), subalarae to mouth distance (7 to 4), inter christa distance (3 to 5), dorsal nasal length (ND; 16 to 11), upper face length (UFL; 16 to 4), full face length, facial width (17 to 18) cranial length (CL; 19 to 20), cranial width (CW) were recorded (Table 1; Figure 1a). Upper face length defined as the vertical distance from the nasion to the lowest point of the crown of an upper central incisor tooth or the lower border of the upper lip. The facial length defined as the distance between nasion and the lowest point of the lower jaw in the mid sagittal plane. The maximum facial width measured in 2D axial or 3D images, at the level of the zygomatic arch, including soft tissues of the face, between lateral most points of the cheek (Fig. 1b). The cranial length measured in 2D sagittal or 3D images (Fig 1c), from glabella to inion—the cranial width measured in axial and sagittal images at the widest point of the skull (Fig. 1d). BOW, ICW, ROW, LOW, REcN, LEcN, AlbW, PronRlb, PronLAl and CW measured from the 2D axial T2 weighted sequence, and 3D reconstructed images. The ND and CL were recorded from the 2D midsagittal image and 3D reconstructed images.

Table 1.
Landmarks and measurements of the face with reference to the 3D reconstructed image of the face (Figure 1)

	Landmarks
Bi-ocular width	12 to 15
Inter-ocular width	13 to 14
Right ocular width	12 to 13
Left ocular width	14 to 15
Right endocanthon to nasion	13 to 16
Left endocanthon to nasion	14 to 16
Alar base width	9 to 10
Pronasalae to right alar-base	9 to 11
Pronasalae to left alar-base	10 to 11
Dorsal nasal length	16 to 11
Subalar width	6 to 8
Subalarae to mouth distance	7 to 4
Mouth width	1 to 2
Inter christa distance	3 to 5
Upper face length	16 to 4
Face length	-
Face width	17 to 18
Cranial length	19 to 20

Mouth width= 1 to 2; 3= right crista philtri; 4= labrare superioris; 5= left crista philtri; 6= right sub alarae; 7= subnasale; 8= left sub alarae; 9= right alarae; 10 = left alarae; 11 = pronasale; 12 = right exo canthum; 13 = right endo canthum; 14 = left endo canthum; 15 = left exo canthum; 16= nasion; 17= right lateral cheek; 18 = left lateral cheek; 19 = gabella; 20 = inion

(The landmarks are defined as 1,2,…ect. with reference to figure 1a)

Fig. 1a.
3D reconstructed MRI image of the face demonstrating facial land marks

Fig. 1b.
Facial width measurement

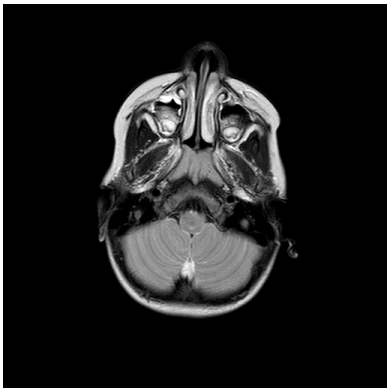

Fig. 1c.
The measurements obtained in sagittal MRI brain

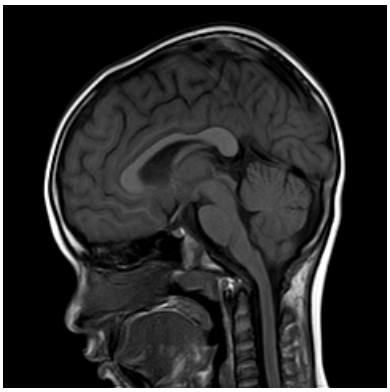

Fig. 1d.
Cranial width measurement

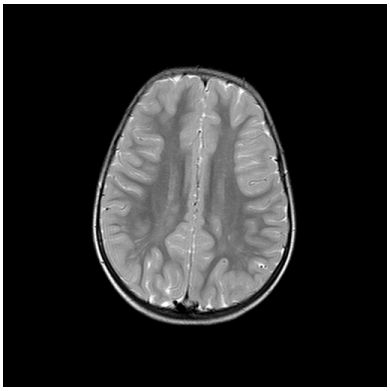

Accuracy of 2D measurements was maintained as follows. The window width was adjusted to 680/1240 to increase the soft-tissue contrast resolution to the maximum; accuracy in defining the landmarks has improved using the split-screen technique by which the measuring points of both axial and sagittal images were synchronized. To maintain the accuracy of the 3D measurements, adequately enlarged images were used to define the landmarks.

After obtaining facial measurements from the brain MRI images done according to the existing protocol, an MRI study that was performed using the proposed protocol to assess the feasibility of proposed protocol (Fig. 2).

Fig. 2.
Three dimensional (3D) reconstructed image of the face obtained by proposed MRI protocol

Statistical analysis

Following normality assessment, the continuous variables were expressed as means and standard deviations; categorical variables were expressed as percentages. Differences between variables were compared using the T-test and the internal integrity of the measurements were assessed by Cronbach's alpha coefficient. The p-values less than 0.05 was considered as significant.

3. Results

The mean age of the study population was 4±2 years with no significant age difference between girls and boys (T=0.044; p=0.966). Table 2 describes the demographic data and facial measurements of the study sample.

Table 2.
Demographic data and 2D facial measurements of the study sample

Measurement	Mean±SD (in cm)	Inter-quartile range
Age	4±2	2.25 – 6.00
Bi-ocular width	8.79±0.54	8.38 – 9.18
Inter-ocular width	2.63±0.23	2.41 – 2.76
Right ocular width	3.10±0.25	2.89 – 3.27
Left ocular width	3.28±0.29	3.09 – 3.52
Right endocanthon to nasion	1.61±0.14	1.47 – 1.70
Left endocanthon to nasion	1.54±0.13	1.44 – 1.63
Alar base width	2.79±0.17	2.64 – 2.90
Pronasalae to right alar-base	2.16±0.24	1.96 – 2.36
Pronasalae to left alar-base	2.15±0.27	1.85 – 2.34
Dorsal nasal length	3.0±0.35	2.55 – 3.29
Upper face length	4.88±0.46	4.78 – 5.32
Face width	9.96±0.6	9.40 – 10.38
Cranial length	16.56±1.0	15.86 – 17.23
Cranial width	13.49±0.77	12.86 – 14.18

Repeatability of measurements

The internal reliability of the measurements was evaluated using Cronbach's alpha coefficient (Table 3). It was found, obtaining facial measurements was reliable with a high intra and inter-observer agreements.

Table.3

Internal reliability of MRI measurements evaluated as intra and inter observer variability

	Intra-observer variability (Chronbach's alpha)	Inter-observer variability (Chronbach's alpha)
Bi-ocular width	0.925	0.971
Inter-ocular width	0.921	0.815
Right ocular width	0.823	0.913
Left ocular width	0.901	0.900
Right endocanthon to nasion	0.894	0.757
Left endocanthon to nasion	0.805	0.909
Alar base width	0.990	0.999
Pronasalae to right alar-base	0.965	0.955
Pronasalae to left alar-base	0.836	0.993
Dorsal nasal length	0.945	0.988
Upper face length	0.941	0.995
Face width	0.957	0.991
Cranial length	0.996	0.994
Cranial width	0.997	0.987

Feasibility of measurements

Table 4 describes the feasibility of obtaining facial measurement using MRI brain images. Facial measurements such as the upper face length and facial width could be obtained in the entire sample (100%) using sagittal and axial images respectively. However, complete facial length measurement was not amenable from both 2D and 3D techniques, since the entire face including the mandible was not contained within the field of view of the brain MRI. Obtaining cranial (cranial length =100%; width = 100%) and ocular measurements (ocular length = 100%; inter-ocular width = 100%; the distance between endocanthon to nasion = 100%) was also feasible for the entire sample. Similarly, upper nasal measurement (dorsal nasal length = 100%) was obtained from the entire sample.

Table 4.

Feasibility of obtaining measurements

	Proportion of studied obtained measurements (2D)	Proportion of studied obtained measurements (3D)
Bi-ocular width	100% (n=20)	100% (n=6)
Inter-ocular width	100% (n=20)	100% (n=6)
Right ocular width	100% (n=20)	100% (n=6)
Left ocular width	100% (n=20)	100% (n=6)
Right endocanthon to nasion	100% (n=20)	100% (n=6)

	Proportion of studied obtained measurements (2D)	Proportion of studied obtained measurements (3D)
Left endocanthon to nasion	100% (n=20)	100% (n=6)
Alar base width	70% (n=14)	100% (n=6)
Pronasalae to right alar-base	70% (n=14)	100% (n=6)
Pronasalae to left alar-base	70% (n=14)	100% (n=6)
Dorsal nasal length	100% (n=20)	100% (n=6)
Subalar width	0% (n=0)	100% (n=6)
Subalarae to mouth distance	0% (n=0)	100% (n=6)
Mouth width	0% (n=0)	100% (n=6)
Inter christa distance	0% (n=0)	100% (n=6)
Upper face length	100% (n=20)	100% (n=6)
Face length	0% (n=0)	0% (n=0)
Face width	100% (n=20)	100% (n=6)
Cranial length	100% (n=20)	100% (n=6)
Cranial width	100% (n=20)	100% (n=6)

The lower part of the nose was not routinely contained in the field of view of axial images. Therefore, the alar base measurements could be obtained only in 70% of the study sample. Basal part of the nose - the root of the alar base (0%) and philtrum (0%) - was not routinely included in the axial imaging field of view, hence not evaluated by the 2D MRI technique. Since this study used sagittal images for 3D image reconstruction, due to an extended field of view, 3D images contained the landmarks of the lower nose (100%) and the upper lip (100%) as well.

The difference between the measurements obtained from 3D and 2D systems were compared and tabulated in Table 5. The 2D and 3D measurements have not shown a significant difference for evaluated craniofacial structures (Table 05).

Table 5.

Comparison of 2D and 3D measurements

	2D measurement	3D measurement	T value	P value
Bi-ocular width	8.79±0.54	8.64±0.33	0.378	0.721
Inter-ocular width	2.63±0.23	2.71±1.89	0.551	0.805
Right ocular width	3.10±0.25	3.12±0.24	0.437	0.680
Left ocular width	3.28±0.29	3.06±0.21	0.411	0.698
Right endocanthon to nasion	1.61±0.14	1.54±0.18	1.331	0.241
Left endocanthon to nasion	1.54±0.13	1.54±0.1	0.903	0408
Alar base width	2.79±0.17	2.88±0.3	1.077	0.360
Pronasalae to right alar-base	2.16±0.24	1.91±0.11	2.478	0.068
Pronasalae to left alar-base	2.15±0.27	1.96±0.25	1.882	0.148
Dorsal nasal length	3.0±0.35	2.82±0.42	1.397	0.122
Subalarae to mouth distance	-	1.16±0.40	-	-
Sn to right Cph	-	1.13±0.17	-	-
Sn to left Cph	-	1.18±0.15	-	-
Right Sbal to left Sbal	-	1.64±0.31	-	-

	2D measurement	3D measurement	T value	P value
Right Sbal to right Cph	-	0.98±0.35	-	-
Left sbal to left Cph	-	1.05±0.31	-	-
Mouth width	-	3.56±0.53	-	-
Upper face length	4.88±0.46	4.70±0.46	1.047	0.343
Face length	-	-	-	-
Face width	9.96±0.6	9.67±0.5	0.728	0.499
Cranial length	16.56±1.0	15.12±83	2.332	0.0.61
Cranial width	13.49±0.77	14.25±1.42	2.369	0.064

(Sn-subnasalae; Ls-labrare superioris; Cph-crista philtri; Sbal-sub alarae;

4. Discussion

Evaluating craniofacial anthropometry is fundamental in successful planning of reconstructive surgeries for facial dysmorphism, and has been done previously using many traditional and novel techniques (Chuang, et al., 2016). Since the MRIs performed in routine brain imaging protocol have not been previously utilized to obtain craniofacial measurements, this study fulfils a timely need of assessing the feasibility and repeatability of a safe and cost-effective novel method. Findings of this study would invariably up-lift the management of facial dimorphisms in children, particularly those who are with cleft lips. Supporting the postulated hypothesis, the results of this study confirm the high reliability in identifying facial landmarks and obtaining measurements using 2D or 3D MRI brain images. Notably, the measurements could be obtained when the intended area is contained in the imaging field of view. Additionally, repeatability of measurements was high as explained by high inter and intra-observer agreements. Since the lower facial landmarks were not routinely included in the field of view of axial sequences (in 2D assessment), the measurements of inferior nasal region and mouth could be readily obtained when using 3D reconstructed images of which such landmarks were contained in the field of view.

The high inter and intra-observer agreement of measurements reported in this study confirms the reliability and repeatability of defining the studied facial landmarks. The findings of this study also prove the capability of obtaining facial measurements by a competent investigator who follows the stated protocol. Since the feasibility of obtaining ocular and upper nasal measurements has reached 100%, the accuracy in defining such landmarks with brain MRI images is confirmed by this study. The reasons for failure in obtaining measurements in the lower face using 2D images could be explained as follows: the field of view (FOV) of a routine axial MRI brain sequence that performed to investigate epilepsy extends from the vertex of the skull to the mastoid process. Therefore, the lower facial structures such as lower nose, mouth or the mandible are included in the FOV. However, the landmarks of the lower face could be assessed using 3D reconstructions of sagittal sequence, because the FOV of the sagittal scans covers most of the face, including a part of the mandible. Importantly, all facial landmarks can be assessed by using a modified MRI protocol with an extended FOV to incorporate the entire face. Therefore, the MRIs done with the proposed extended FOV protocol will allow pre-surgical evaluation of lower facial structures such as alar base, philtrum, orbicularis oris muscle, and mouth as well (Whittle, 2004).

The field of view (FOV) of the MRI is inversely related to the contrast resolution and image quality (David & Yousem, 2010; Reeth EV, et al., 2014). Therefore, unjustifiable increments in the FOV would

results in low-quality images, adversely affecting the measurement accuracy as well. However, since children have a considerably small facial surface area, their entire face would possibly be contained within a small FOV without affecting the image quality. Anyhow, technological improvements, such as using a surface coil, may be required to maintain the image quality when the FOV is more extensive such as in teenager or adults (Chakravarty, et al., 2011).

Facial dysmorphic syndromes and cleft lip deformity are often associated with cleft palate and abnormalities in periorbital soft tissues, such as in per orbital skin, orbicularis oris muscle, and premaxilla (Paranaíba, et al., 2011; Paranaíba, et al., 2013; Neiswanger, et al., 2007; Marazita, 2007). Neither the traditional assessment techniques - cephalometry, imprinted moulds or photography - nor the novel techniques, such as 3D photographic methods, do not facilitate the assessment of periorbital soft tissues (Johnston & Chazal, 2018; Çeliktutan, et al., 2013; Othman, et al., 2016). In contrast, MRI images of the brain have an excellent soft-tissue differentiating ability, thus visualize additional anatomical details facilitating a successful reconstructive surgery. Further, much needed detailed palatal and mid-facial anatomy can also be obtained using MRI brain images (David & Yousem, 2010; Reeth EV, et al., 2014).

Few studies have evaluated the craniofacial anthropometry using 3D reconstructed facial MRI images, of which the 3D reconstruction has performed using a modified imaging protocol, where 1mm brain slices were obtained using a T1 weighted sagittal sequence (Daboul, et al., 2018; Vivian SL, 2005). In routine MRI brain protocol, the slice thickness set to 5 mm. Though we could obtain measurements successfully with 3D reconstructed images from 5 mm brain slices, it has stated that 3D reconstructions performed with slices thicker than 1 mm are not optimum for such purposes due to stair-step artefact. The stair-step artefact may interfere with the accuracy of obtaining body surface measurements (Yoon JH, et al., 2019). Such artefacts could be prevented by modifying the MRI protocol and performing sagittal sequence at 1 mm slice thickness (Fig. 1).

Compared to other imaging techniques, the time required to perform an MRI study is more extensive, thus considered as a significant limitation. Image artefacts on patient movements (motion artefacts) is another limitation of MRI. In order to prevent motion artefacts, the patient needed to be motionless throughout the procedure. Therefore, the duration of the scan is a crucial factor for children (Reeth EV, et al., 2012; Yoon JH, et al., 2019). The scanning time is proportionate to the number of image sequences performed (Yoon JH, et al., 2019). Out of many brain MRI image sequences, the current study has included only the axial T2 weighted and sagittal T1weighted sequences, hence can be considered as a relatively limited time-consuming protocol. Short duration MRI protocols have many advantages. Firstly, a study that can be performed within a few minutes is preferable for children, as it requires only light sedation to keep them motionless (Arlachov & Ganatra, 2012). Secondly, this modified protocol has the ability to delineate the majority of intracranial pathologies within a few minutes. Therefore, this protocol is valuable as a screening tool (David & Yousem, 2010; Reeth EV, et al., 2014). Thirdly, MRI imaging technique can be considered as a low-risk procedure considering the non-invasive nature and lack of exposure to ionizing radiation. Therefore, executing MRI images of the brain for simultaneous evaluation of craniofacial measuremtns and intracranial anomalies can be considered as a rational approach.

The cleft lip is the most common craniofacial malformation. The optimum timing for surgical repair of cleft lip is a widely discussed topic with a wide variation in recommendations. Recommendations vary from early surgery - before six months to get maximum speech outcome, to surgical intervention after the completion of maxillary growth (Tettamanti, et al., 2017). Considering such debates on

optimum timing of the surgery, we have selected the study sample with a wide age range to cover all possible ages that might need surgical interventions.

The current study can be regarded as a pioneer study that describes a novel methodology to obtain craniofacial measurements from MRI brain images for children with craniofacial malformations. However, the study suffers from several limitations. Since this is a pilot study that defines a suitable imaging protocol to obtain facial measurements from MRI brain scans, further testing of the protocol is recommended using a larger sample with a wide age distribution. Also, it is recommended to validate the MRI measurements by comparing them with direct facial measurements obtained by a caliper.

In conclusion, MRI brain scans performed to evaluate cerebral pathology can be successfully executed to evaluate facial measurements, provided the field of view of the brain scan is adjusted to include all significant landmarks of the face. Both 2D and 3D MRI brain images provided a sufficient platform for surface measurements. Brain scan performed with an extended field of view, at 1 mm slice thickness, can be proposed as the facial imaging protocol for craniofacial malformations.

5. Conflicts of interest

no

6. Funding

self funded

References

Agbenorku P. (2013) Orofacial Clefts: A Worldwide Review of the Problem. Int Sch Res Notices; ID 348465. http://dx.doi.org/10.5402/2013/348465

Arlachov Y, Ganatra RH.(2012) Sedation/anaesthesia in paediatric radiology. Br J Radiol (1019):e1018-e1031. https://doi.org/10.1259/bjr/28871143

Barrera JE. (2011) Addressing Challenges of Cleft Lip and Palate Deformity in Afghanistan. *Arch Facial Plast Surg.* https://doi.org/10.1001/archfacial.2011.70

Bekele KK, Ekanem PE. (2019) Anatomical patterns of cleft lip and palate deformities among neonates in Mekelle, Tigray, Ethiopia; implication of environmental impact. BMC pediatric. https://doi.org/10.1186/s12887-019-1624-2

Campbell A, Costello B, Ruiz R. (2010) Cleft lip and palate surgery: An update of clinical outcomes for Primary Repair. Oral Maxillofac Surg Clin NA. https://doi.org/10.1016/j.coms.2009.11.003

Çeliktutan O, Ulukaya S, Sankur B. (2013) A comparative study of face landmarking techniques. Eurasip J Image Video Process. https://doi.org/10.1186/1687-5281-2013-13

Chakravarty MM, Aleong R, Leonard G, at al. (2011) Automated Analysis of Craniofacial Morphology Using Magnetic Resonance Images. PLoS ONE. https://doi.org/10.1371/journal.pone.0020241

Chuang J, Barnes C, Wong B. (2016) Overview of Facial plastic surgery and current developments. Surg J. https://dx.doi.org/10.1055%2Fs-0036-1572360

Daboul A, Ivanovska T, Bu R, et al. (2018) Procrustes-based geometric morphometrics on MRI images: An example of inter-operator bias in 3D landmarks and its impact on big datasets. PLoS ONE: e0197675. https://doi.org/10.1371/journal.pone.0197675

David M, Yousem MD. (2010) Neuroradiology: the requisites Elsiever USA. https://www.elsevier.com/books/neuroradiology-the-requisites/nadgir/978-1-4557-7568-2

Fakhim SA, Shahidi N, Lotfi A. (2016) Prevalence of Associated Anomalies in Cleft Lip and / or Palate Patients. Iran J Otolaryngology. https://pubmed.ncbi.nlm.nih.gov/27280100/

Farkas LG (1994) Anthropometry of the head and face. 2nd ed., New York: Raven Press.

Johnston B, Chazal P de. (2018) A review of image-based automatic facial landmark identification techniques. Eurasip J Image Video Process. https://doi.org/10.1186/s13640-018-0324-4

Marazita M. (2007) Subclinical features in non-syndromic cleft lip with or without cleft palate (CL/P): review of the evidence that subepithelial orbicularis oris muscle defects are part of an expanded phenotype for CL/P. Craniofac Res. https://doi.org/10.1111/j.1601-6343.2007.00386.x

de Menezes M, Sforza C. (2010) Three-dimensional face morphometry. Dental Press J Orthod. https://www.scielo.br/pdf/dpjo/v15n1/en_02.pdf

Moss J, Linney A, Grindrod S. Arridge S, Clifton J (1987) Three-dimensional visualization of the face and skull using computerized tomography and laser scanning techniques. Eur J Orthod. https://doi.org/10.1093/ejo/9.4.247

Neiswanger K, Weinberg SM, Rogers CR, et al. (2007) Orbicularis oris muscle defects as an expanded phenotypic feature in non-syndromic cleft lip with or without cleft palate. Am J Med Genet A. https://doi.org/10.1002/ajmg.a.31760

Nopoulos P, Langbehn DR, Canady J, at al. (2007) Abnormal Brain Structure in Children with Isolated Clefts of the Lip or Palate. *Arch Pediatr Adolesc Med.* https://ja.ma/3bCMwEY

Nopoulos P, Berg S, Van Demark D, et al. (2001) Increased Incidence of a Midline Brain Anomaly in Patients with Non syndromic Clefts of the Lip and/or Palate. J Neuroimaging. https://doi.org/10.1111/j.1552-6569.2001.tb00072.x

Othman, S., Aidil Koay, N. (2016) Three-dimensional facial analysis of Chinese children with repaired unilateral cleft lip and palate. Sci Rep 6, 31335. https://doi.org/10.1038/srep31335

Osborn AG. (2017) Osborn's brain: imaging, pathology and anatomy. 2nd ed.; Elsevier - Health Sciences Division, Philadelphia, USA. https://www.elsevier.com/books/osborns-brain/osborn/978-0-323-47776-5

Paranaíba LMR, Miranda RT de, Ribeiro LA, et al. (2011) Frequency of congenital craniofacial malformations in a Brazilian Reference Center. Rev Bras Epidemiol. https://doi.org/10.1590/S1415-790X2011000100014

Reeth EV, Tham IWK, Tan CH, Poh CLOO. (2012) Super-Resolution in Magnetic Resonance Imaging: A Review. Concept Magn Reson A. https://doi.org/10.1002/cmr.a.21249

Ribeiro P, Ladeira S De, Alonso N. (2012) Protocols in Cleft Lip and Palate Treatment: Systematic Review. Plast Surg Int; ID 562892 https://doi.org/10.1155/2012/562892

Shkoukani MA, Chen M, Vong A. (2013) Cleft lip – a comprehensive review. Front Pediatric. https://doi.org/10.3389/fped.2013.00053

Tettamanti L, Avantaggiato A, Nardone M, at al. (2017) Cleft palate only: current concepts. Oral Implantol (Rome). https://dx.doi.org/10.11138%2Forl%2F2017.10.1.045

Tettamanti L, Avantaggiato A, Nardone M, Tagliabue A (2017) A cleft palate only: current concepts. Oral and implanol. https://dx.doi.org/10.11138%2Forl%2F2017.10.1.045

Venkatesh R. (2009) Syndromes and anomalies associated with cleft. Indian J Plast Surg. Suppl https://dx.doi.org/10.4103%2F0970-0358.57187

Vivian SL. (2005) Cardiovascular MRI: Physical principals to practical protocols. Lippincott Williams & Wilkins. https://www.ovid.com/product-details.5143.html

Whittle J. (2004) Preoperative anthropometric analysis of the cleft child's face: A comparison between groups. Int J Surg. https://doi.org/10.1016/S1743-9191(06)60051-4

Yoon JH, Nickel MD, Peeters JM, et al. (2019) Rapid Imaging: Recent Advances in Abdominal MRI for Reducing Acquisition Time and Its Clinical Applications. Korean J Radiol. https://dx.doi.org/10.3348%2Fkjr.2018.0931

RESUMEN

La evaluación prequirúrgica de la morfometría facial con frecuencia se justifica para niños con dismorfismo facial. Aunque muchos métodos se utilizaron anteriormente para tales fines, los datos son escasos sobre el uso de imágenes cerebrales por resonancia magnética (MRI) para tales fines. El propósito de este estudio fue evaluar la viabilidad de utilizar resonancias magnéticas cerebrales realizadas en el protocolo de imágenes de epilepsia para evaluar la morfometría facial.

Medidas de la cara, la órbita, la boca y la nariz de niños de 1 a 7 años se obtuvieron mediante imágenes de resonancia magnética cerebral T1 sagital, axial T2 y tridimensional (3D) del cerebro (n = 20). Se obtuvieron las medidas faciales, y fue calculada la variabilidad inter e intraobservador.

La edad de los niños estudiados fue de 4 ± 2 años, de los cuales el 40% (n = 8) hombre y el 60% (n = 12) mujer. La obtención de medidas faciales fue confiable con altos acuerdos intraobservador (α = 0,757 a 0,999) e interobservador (α = 0,823 a 0,997). Los puntos de referencia del cráneo, la cara superior y la nariz superior se pudieron identificar (100%) tanto en imágenes bidimensionales (2D) como en 3D cuando dichos puntos de referencia estaban contenidos en el campo de visión de la imagen (FOV). Los puntos de referencia de la parte inferior de la nariz (ancho subalar = 0%) o la boca (0%) no estaban contenidos en el campo de visión de las imágenes 2D, sino que estaban contenidos en las imágenes 3D (100%). Tanto las imágenes 2D como las 3D no permitieron la evaluación de la parte inferior de la cara o la mandíbula, ya que tales puntos de referencia no estaban contenidos en el campo de visión.

Concluimos que las resonancias magnéticas cerebrales realizadas para evaluar la patología cerebral se pueden usar para evaluar las medidas faciales, siempre que el campo de visión de la exploración se ajuste para incluir todos los puntos de referencia importantes.

Palabras clave: Malformaciones craneofaciales; niños; medidas faciales; factibilidad; resonancia magnética cerebral.